

Nested Cavity Classifier: performance and remedy[☆]

Waleed A. Mustafa^a, Waleed A. Yousef^{b,*}

^aB.Sc., TU Kaiserslautern: Technische Universität Kaiserslautern

^bPh.D., Associate Professor, Computer Science Department, Faculty of Computers and Information, Helwan University, Egypt.
Director, Human Computer Interaction Laboratory (HCI Lab.)

Abstract

Nested Cavity Classifier (NCC) is a classification rule that pursues partitioning the feature space, in parallel coordinates, into convex hulls to build decision regions. It is claimed in some literatures that this geometric-based classifier is superior to many others, particularly in higher dimensions. First, we give an example on how NCC can be inefficient, then motivate a remedy by combining the NCC with the Linear Discriminant Analysis (LDA) classifier. We coin the term Nested Cavity Discriminant Analysis (NCDA) for the resulting classifier. Second, a simulation study is conducted to compare both, NCC and NCDA to another two basic classifiers, Linear and Quadratic Discriminant Analysis. NCC alone proves to be inferior to others, while NCDA always outperforms NCC and competes with LDA and QDA.

Keywords: Classification, Nested Cavity Classifier (NCC), Parallel Coordinates.

1. Introduction

Nested Cavity Classifier (NCC) is a geometric-based classification rule that pursues partitioning the feature space in parallel coordinates (abbreviated ||-coords) into convex-hulls to build decision regions (Inselberg and Avidan, 2000). Many articles and books considered the assessment of classifiers using simulated and real-world datasets (e.g., (Raudys and Pikelis, 1980; Efron and Tibshirani, 1997; Hastie et al., 2001)); but none of them considered a systematic assessment of NCC. However, Inselberg and Avidan (2000) compared NCC with other classifiers only on few real high-dimensional datasets; that study mentioned the superiority of NCC over other classifiers.

NCC, as described below, builds decision regions geometrically using convex hulls. This partitioning mechanism has a drawback on the performance of the NCC (as explained in Section 3). NCC classifies any testing observation—regardless to its class, whether “class 1” or “class 2”—as class, say, “class 2” as long as it does not lie inside the range of the training data set; i.e., within the minimum and maximum values of each dimension. Since this is not always true, the present article proposes combining NCC with LDA to classify observations outside the range of the training set. We coin “Nested Cavity Discriminant Analysis (NCDA)” as a name for the resulting classifier.

The present article is organized as follows. Section 3 explains the NCC. Section 4 motivates combining NCC with LDA. Section 5 is a simulation study that compares NCC and NCDA to other classifiers. Section 6 is a conclusion and a discussion for future work.

2. Parallel Coordinates (||-Coords)

Data visualization can inspire one to solve very complex problems. When data is visualized, inter-variable relations can be easily spotted; these relations are patterns. Detecting these patterns is a pattern recognition problem. We usually map problems into geometrical space; and by using the amazing pattern recognition capabilities of our eyes and brains we try to figure things out.

Mapping a problem into the ordinary geometrical space involves mapping variables into corresponding space axes (orthogonal axes). A problem arises when there is a need to visualize high dimensional data because we are only familiar with 3 dimensional orthogonal space. This confines us to visualize only 3-dimensional problems, which is not sufficient in real-life situations. Said differently, “orthogonal visualization uses up the plane very quickly” Inselberg (2002).

Orthogonality, depending on the notion of an “angle”, inspired “Maurice d’Ocagne” in 1885, who realized that if we could represent the problem into axes without the need for an angle we will not use orthogonal axes. This implies that we will not use up the plane that quickly. Since the opposite of orthogonality is parallelism, representing the problem in a geometric form by mapping the variables into parallel axes rather than orthogonal axes will help us to visualize high dimensional problems.

[☆]This manuscript was initially composed in 2009 as part of a research pursued that time. This paper is currently under consideration in Pattern Recognition Letters.

* Corresponding Author

Email addresses: WaleedAMustafa@gmail.com (Waleed A. Mustafa), wyousef@GWU.edu, wyousef@fci.helwan.edu.eg (Waleed A. Yousef)

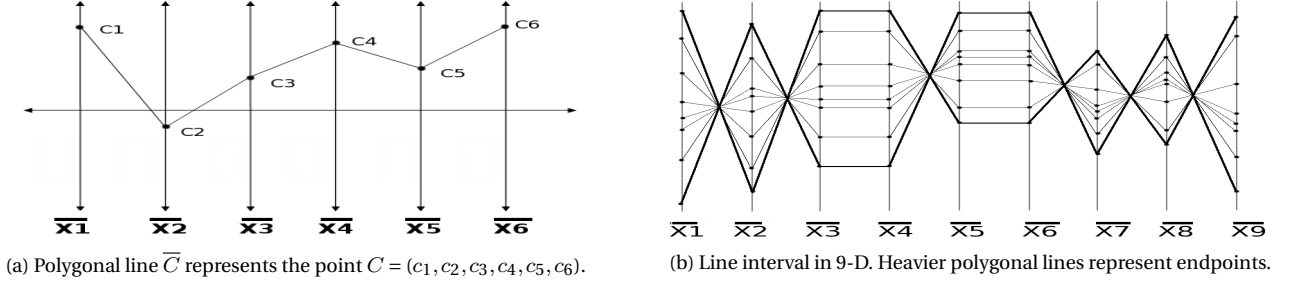


Figure 1: Parallel Coordinates.

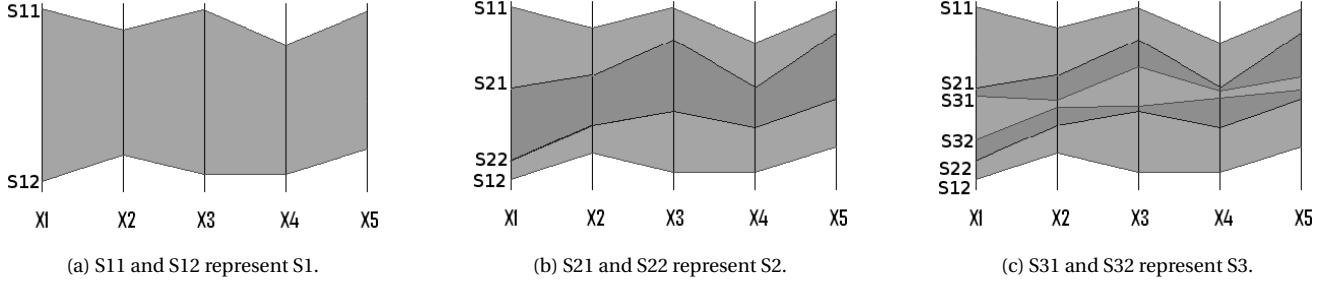


Figure 2: Three regions built successively by NCC in ||-coords.

3. Nested Cavity Classifier (NCC)

We first consider the binary classification problem, where an observation $t_i = (x_i, y_i)$ has the p -dimensional feature vector x_i (the predictor), and the response is y_i . The response y_i equals one of the two classes, ω_1 or ω_2 . Assume the availability of a training dataset $\mathbf{t} = \{t_i : t_i = (x_i, y_i), i = 1, \dots, n\}$. This data set is used to learn the geometrical structure of the problem and to design a classification rule $\eta_{\mathbf{t}}$. For any future observation having a feature vector x_0 and an unknown class, the task of $\eta_{\mathbf{t}}$ is to predict the class y_0 , i.e., to provide the prediction $\eta_{\mathbf{t}}(x_0)$, which equals ω_1 or ω_2 .

The process of learning from data and choosing a model for building $\eta_{\mathbf{t}}$ should be preceded by data visualization, which provides a very useful insight to select the right model. NCC works on the visualized version of the training data set represented in ||-coords to build hyper decision surfaces (Inselberg, 2002; Inselberg and Avidan, 2000; Chen et al., 2008). In the following paragraph we give a very brief account for ||-coords, then explain how NCC works.

In X - Y Cartesian coordinates, p copies of real lines labeled $\bar{X}_1, \bar{X}_2, \dots, \bar{X}_p$ are placed equidistantly and perpendicular to the X -axis. These are the axes of the Parallel Coordinate system for \mathcal{R}^p Euclidean space. A point C with coordinates (c_1, c_2, \dots, c_p) is represented by the complete polygonal line \bar{C} , whose p vertices are at $(i-1, c_i)$ on the X_i -axis, $i = 1, \dots, p$ as shown in Figure 1-a. In this way, a 1-1 correspondence between points in \mathcal{R}^p and planar polygonal lines in X - Y Cartesian coordinates is established (Inselberg (2002)). For Example, Figure 1-b shows another example, a line segment in 9 dimensions by showing 8 points on this segment including the two endpoints. This kind of data representation is impossible in the perpendicular coordinates.

In ||-coords, a dataset with p variables and n observations is represented by a set of 2-dimensional points. The total number of those points equals $p \times n$. With the dataset represented this way, we use an efficient convex-hull approximation algorithm to wrap (i.e., create an approximate convex-hull) the points of, say, ω_1 . At this point we have created a hyper surface S_1 that contains all observations of ω_1 and some observations of ω_2 as well (Figure 2-a). We then apply convex-hull approximation to the set of points of ω_2 that are enclosed within the hyper surface S_1 to produce the hyper surface S_2 (Figure 2-b). We repeat this process successively till the maximum complexity required is reached (i.e. the maximum number of inner convex-hulls); this is usually used as a regularization parameter to guard against overtraining.

After the algorithm terminates, the description of the hyper surface that represents the decision region of ω_1 is formalized as

$$S_{\omega_1} = \begin{cases} (S_1 - S_2) \cup (S_3 - S_4) \dots \cup (S_{m-1} - S_m) & \text{if } m \text{ is even} \\ (S_1 - S_2) \cup (S_3 - S_4) \dots \cup S_m & \text{if } m \text{ is odd,} \end{cases} \quad (1)$$

where S_m is the last produced hyper surface. Hence, for a given future observation x_0 , the classification rule $\eta_{\mathbf{t}}^{(NCC)}$ is formalized as follows.

$$\eta_{\mathbf{t}}^{NCC}(x_0) = \begin{cases} \omega_1 & \text{if } x_0 \in S_{\omega_1} \\ \omega_2 & \text{otherwise} \end{cases} \quad (2)$$

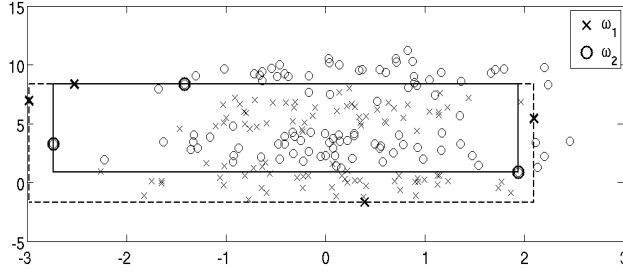


Figure 3: Decision regions built by NCC in ||-coords and displayed in orthogonal coordinates. The dashed boundary represents S_1 and the solid represents S_2 . The bold observations are those used to build the boundary.

4. Combining LDA with NCC: a remedy

As described in section 3, NCC uses a geometric criterion to build the decision regions. The rule $\eta_{\mathbf{t}}^{(NCC)}$ in (2) implies that

$$\eta_{\mathbf{t}}^{(NCC)}(x_0) = \omega_2 \quad \forall x_0 \notin S_1. \quad (3)$$

This means that all test observations belonging to ω_1 and lying outside S_1 will be misclassified!

Figure 3 illustrates decision regions built by NCC. The dashed rectangle represents S_1 and the solid rectangle represents S_2 . The observations used for building these surfaces are plotted in bold. Notice that any observation $x_0 (= (x_{01}, x_{02}))$ located outside the boundaries of S_1 will be classified as $\eta_{\mathbf{t}}^{(NCC)}(x_0) = \omega_2$. However, from the data plot, x_0 is most probably belonging to ω_1 if $x_{02} < -2.2$ (the lower boundary of S_1).

This was the motivation behind combining NCC with any other statistical rule. Such a combination will provide the means for learning how to classify future observations located outside the outer surface S_1 . We chose the Linear Discriminant Analysis (LDA) for demonstration; however we could have chosen the Quadratic Discriminant Analysis (QDA) or any other discriminant function, hence the name Nested Cavity Discriminant Analysis (NCDA). However, since the aim behind this combination is to be able to classify observations from the tail of the data distribution, we think that LDA or QDA will be quite sufficient.

The proposed classification rule is simple; we train NCC using the data set \mathbf{t} to learn the geometric structure and build the decision rule $\eta_{\mathbf{t}}^{(NCC)}$. LDA is also trained with \mathbf{t} to build the decision rule $\eta_{\mathbf{t}}^{(LDA)}$. The final classification rule $\eta_{\mathbf{t}}^{(NCDA)}$ will be

$$\eta_{\mathbf{t}}^{(NCDA)}(x_0) = \begin{cases} \eta_{\mathbf{t}}^{(NCC)}(x_0) & \text{if } x_0 \in S_1 \\ \eta_{\mathbf{t}}^{(LDA)}(x_0) & \text{otherwise,} \end{cases} \quad (4)$$

5. Simulation and Discussion

A simulation study is conducted to compare NCC, NCDA, LDA, and QDA. several simulation parameters should be considered; however, the purpose of the present article is to provide a preliminary simulation study rather than a comprehensive one—refer to Section 6 for future work currently in progress. The data distributions F_1 and F_2 are assumed to be normals and mixture of normals (with parameters discussed below), dimensionality p is chosen to be 2, 4, 8 and 16, and size of the training set, n , is chosen to be 10, 20, 40, 80, 160 and 200 (assuming equal training set sizes for the two classes).

We conducted three sets of experiments; in each experiment we train the classifier on a finite training set (of the selected size n), and test on a testing set of size 1000 observations per class to mimic the population. Each training and testing represents one Monte-Carlo (MC) trial. We typically use 1000 MC trials; in each we train on a different training set (of the same size) drawn from the same population and test on the same 1000-observation-per-class testing set.

We measure the performance in terms of error rate Err . The population parameters of interest, then, are the mean (over the training sets of the same size) performance $E_{\mathbf{tr}} Err$ and the variance $\text{Var}_{\mathbf{tr}} Err$. For each experiment we plot the mean and the standard deviation of the performance versus the reciprocal of the training set size.

The first set of experiments assumes F_1 and F_2 to be multinormal. The mean vector μ_1 is set to zero vector and the mean vector μ_2 is set to $c\mathbf{1}$, where $\mathbf{1}$ is a vector whose all components are equal to 1 and c is a constant that can be used to adjust the classes separability; for our current simulation study we set it to 1. Covariance matrices are set to identity matrix. Figure 4 presents the results of this configuration.

The figure illustrates the typical performance of the LDA and QDA that is well known in the literature; (e.g., see Chan et al., 1998). The LDA is the winner if compared to the other three, since it is the Bayes classifier for this configuration. However, the NCC behaves the other way around for low dimensionality; its performance deteriorates as the training set size increases! The interpretation of these results is interesting. For simplicity, consider the case of $p = 2$; the two distributions will look like two circular clouds, one centered at the origin and the other is centered at (c, c) . With very small training data set, we can imagine that the mean decision surface is a square centered at the origin and enclosed within the first cloud. This will lead to a misclassification for all the testing observations coming from F_1 and occur outside the square.

Increasing the training set size gives a chance to more training observations to occur at the tail of the distribution. Hence, this will widen the decision surface (the square)—refer to Section 3 for information on how NCC works; this decreases the misclassification rate from the first distribution. Therefore, the performance will increase with the training sample size until the decision surface encloses—roughly speaking—the first cloud, yet, did not intersect with the second cloud. Increasing the training sample size more will allow the decision surface to grow until it intersects with the second cloud, the time at which the second type of error will increase.

The improvement of NCDA over the NCC is evident for all dimensions and for all sample sizes; even, it comes closer to the LDA for higher dimensions.

The second set of experiments assumes F_1 to be a mixture of two Gaussians, named F_{11} and F_{12} , with identity covariance matrices and mean vectors $\mu_{11} = \mathbf{0}$ and $\mu_{12} = 2c\mathbf{1}$ respectively. F_2 is assumed to be normal with identity covariance matrix and $\mu_2 = c\mathbf{1}$; we set $c = 1$. This means that F_1 is symmetric bimodal and F_2 is symmetric and lying between the two bumps of F_1 . Figure 5 presents the results of this configuration.

The flat performance of the LDA at 0.5 error rate is not a surprise; this is due to the fact that the problem is symmetric and the hyper plane of symmetry, which will be the decision surface, divides each distribution into two regions each has 0.5 probability. The QDA is the winner for its ability to build quadratic surfaces capable of surrounding observations from F_2 . In this configuration the performance of the NCC gets worse as the dimensionality increases. This is in contrast to the results of the first configuration. Moreover, at some training set sizes we get $E_{\text{tr}} \text{Err} > 0.5$, which means that the NCC rule has to be flipped to produce a mean error rate of $1 - E_{\text{tr}} \text{Err} < 0.5$. Therefore, the sign of the rule varies with the training set size! and has to be determined by estimating the error rate using one of the resampling techniques, e.g., cross validation. We can also notice that NCDA outperforms NCC universally.

The third set of experiments assumes both F_1 and F_2 to be a mixture of two Gaussians (with two different mean vectors and same identity covariance matrix). The first mean vector of F_1 , μ_{11} , is set to zero vector. The second mean vector of F_1 , μ_{12} , is set to $2c\mathbf{1}$. The first mean vector of F_2 , μ_{21} , is set to $c\mathbf{1}$. The second mean vector of F_2 , μ_{22} , is set to $3c\mathbf{1}$; again, we chose $c = 1$. Figure 6 presents the results of this configurations.

From the figure we can observe that NCC, in the majority of experiments, is inferior to the other three classifiers, while the NCDA outperforms all of them in many cases (except at $p = 2$).

6. Conclusion and future work

In this article we introduced a modification on the NCC classifier by combining it with the LDA; we coined the name NCDA on the new classifier. We established a preliminary simulation study to compare the performance of the NCC and NCDA to two basic classifiers, LDA and QDA. Our simulation study reveals that the NCC is inferior to all other three classifiers almost at all considered dimensions, training sample sizes, and distributions. This is in contrast to what has been reported in some literatures (e.g., [Inselberg, 2002](#)). Our proposed classifier, NCDA, outperforms NCC in all experiments; moreover, it outperforms both LDA and QDA in some experiments.

Our future work, currently under progress in our group, considers several points. First, we are planning for more comprehensive simulation study for more understanding of the behavior of NCC and NCDA. Second, we always advocate for using the Area Under the receiver operating characteristic Curve (AUC) (see, e.g., [Hanley and McNeil, 1982](#)) as a performance measure, since it is independent of the threshold at which we make our decision. However, in the present article, we measure the performance of a classifier in terms of the error rate for two reasons. (1) error rate is the performance measure that was used in [Inselberg \(2002\)](#) to compare the NCC to other classifiers. (2) measuring the performance in terms of the AUC only suits a classifier whose output is given in terms of quantitative scores rather than binary decisions as NCC and NCDA. The work currently under progress in our group is considering converting the NCC, and its smarter version NCDA, to score-based classifiers to allow us to assess them in terms of the AUC ([Yousef, 2019a,d, 2013](#)). In addition, we have the opportunity to apply a whole literature of nonparametric estimation procedures including our methods: estimating uncertainty using influence function ([Yousef et al., 2005](#)), estimating uncertainty using UMVU estimation ([Yousef et al., 2006; Chen et al., 2012b,a](#)), and estimating uncertainty using cross validation estimators ([Yousef, 2019c,b](#)), among others.

References

- Chan, H.P., Sahiner, B., Wagner, R.F., Petrick, N., 1998. Effects of Sample Size on Classifier Design for Computer-Aided diagnosis. *Medical Imaging 1998: Image Processing, Pts 1 and 2* 3338, 845–858 1574.
- Chen, C.h., Härdle, W., Unwin, A., 2008. *Handbook of data visualization*. Springer, Berlin.
- Chen, W., Gallas, B.D., Yousef, W.A., 2012a. Classifier Variability: Accounting for Training and testing. *Pattern Recognition* 45, 2661–2671. URL: <https://doi.org/10.1016/j.patcog.2011.12.024>, doi:10.1016/j.patcog.2011.12.024.
- Chen, W., Yousef, W.A., Gallas, B.D., Hsu, E.R., Lababidi, S., Tang, R., Pennello, G.A., Symmans, W.F., Pusztai, L., 2012b. Uncertainty Estimation With a Finite Dataset in the Assessment of Classification models. *Computational Statistics & Data Analysis* 56, 1016–1027. doi:10.1016/j.csda.2011.05.024.
- Efron, B., Tibshirani, R., 1997. Improvements on Cross-Validation: the .632+ Bootstrap Method. *Journal of the American Statistical Association* 92, 548–560.
- Hanley, J.A., McNeil, B.J., 1982. The Meaning and Use of the Area Under a Receiver Operating Characteristic ({ROC}) curve. *Radiology* 143, 29–36.
- Hastie, T., Tibshirani, R., Friedman, J.H., 2001. *The elements of statistical learning: data mining, inference, and prediction*. Springer, New York.

- Inselberg, A., 2002. Visualization and Data Mining of High-Dimensional data. *Chemometrics and Intelligent Laboratory Systems* 60, 147.
- Inselberg, A., Avidan, T., 2000. Classification and visualization for high-dimensional data. URL: <https://doi.org/http://doi.acm.org/10.1145/347090.347170>, doi:<http://doi.acm.org/10.1145/347090.347170>.
- Raudys, S., Pikelis, V., 1980. On Dimensionality, Sample Size, Classification Error, and Complexity of Classification Algorithm in Pattern Recognition. *Pattern Analysis and Machine Intelligence, IEEE Transactions on PAMI-2*, 242–252.
- Yousef, W.A., 2013. Assessing Classifiers in Terms of the Partial Area Under the Roc curve. *Computational Statistics & Data Analysis* 64, 51–70. URL: <https://doi.org/10.1016/j.csda.2013.02.032>.
- Yousef, W.A., 2019a. AUC: nonparametric estimators and their smoothness. arXiv preprint arXiv:1907.12851.
- Yousef, W.A., 2019b. Estimating the standard error of cross-validation-based estimators of classification rules performance. arXiv preprint arXiv:1908.00325.
- Yousef, W.A., 2019c. A leisurely look at versions and variants of the cross validation estimator. arXiv preprint arXiv:1907.13413.
- Yousef, W.A., 2019d. Prudence when assuming normality: an advice for machine learning practitioners. arXiv preprint arXiv:1907.12852.
- Yousef, W.A., Wagner, R.F., Loew, M.H., 2005. Estimating the Uncertainty in the Estimated Mean Area Under the {ROC} Curve of a Classifier. *Pattern Recognition Letters* 26, 2600–2610.
- Yousef, W.A., Wagner, R.F., Loew, M.H., 2006. Assessing Classifiers From Two Independent Data Sets Using {ROC} Analysis: a Nonparametric Approach. *Pattern Analysis and Machine Intelligence, IEEE Transactions on* 28, 1809–1817.

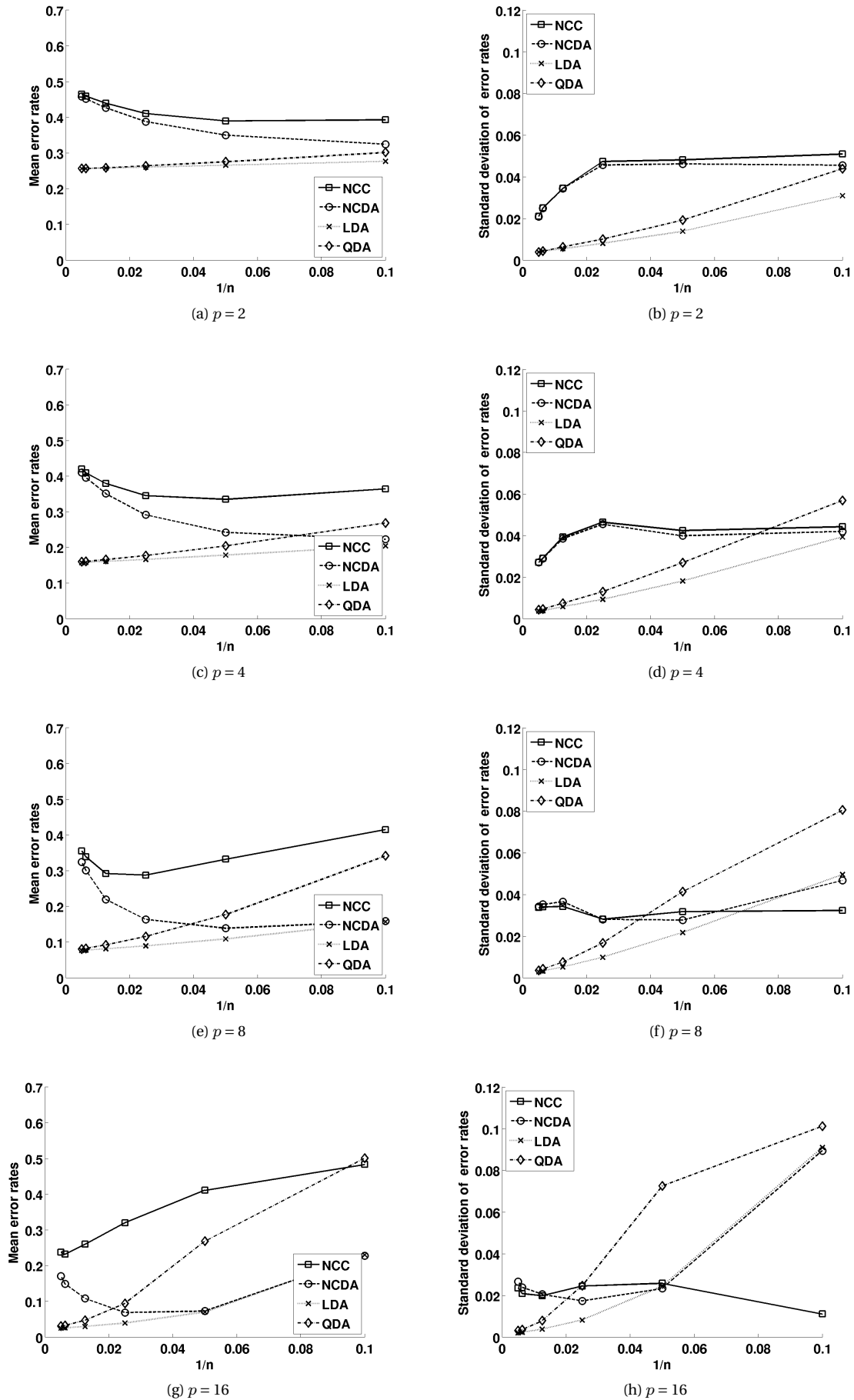


Figure 4: Experiment 1 (multinomial distribution): Mean (left) and standard deviation (right) of error rate under different p .

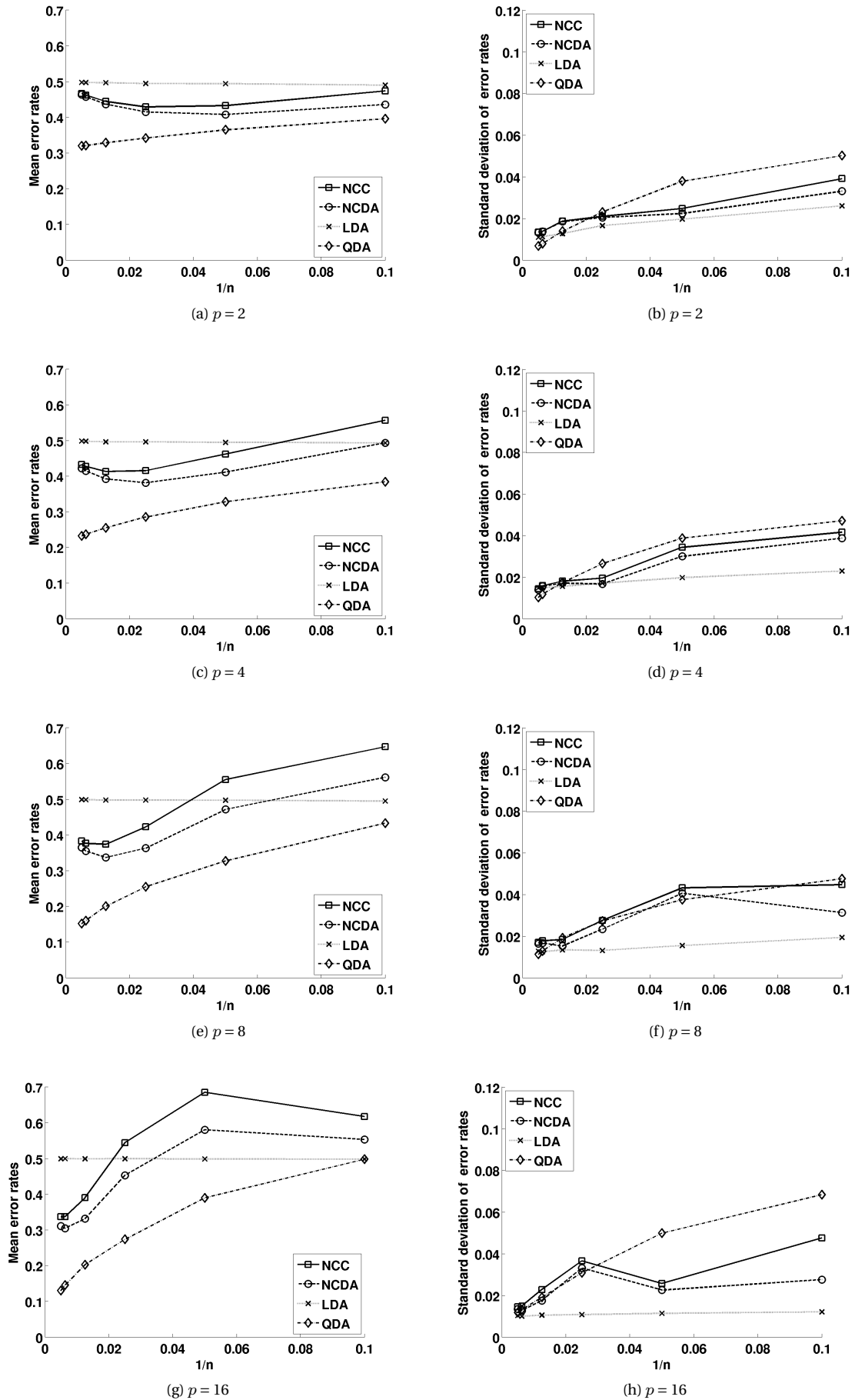


Figure 5: Experiment 2 (mixture of two Gaussians): Mean (left) and standard deviation (right) of error rate under different p .

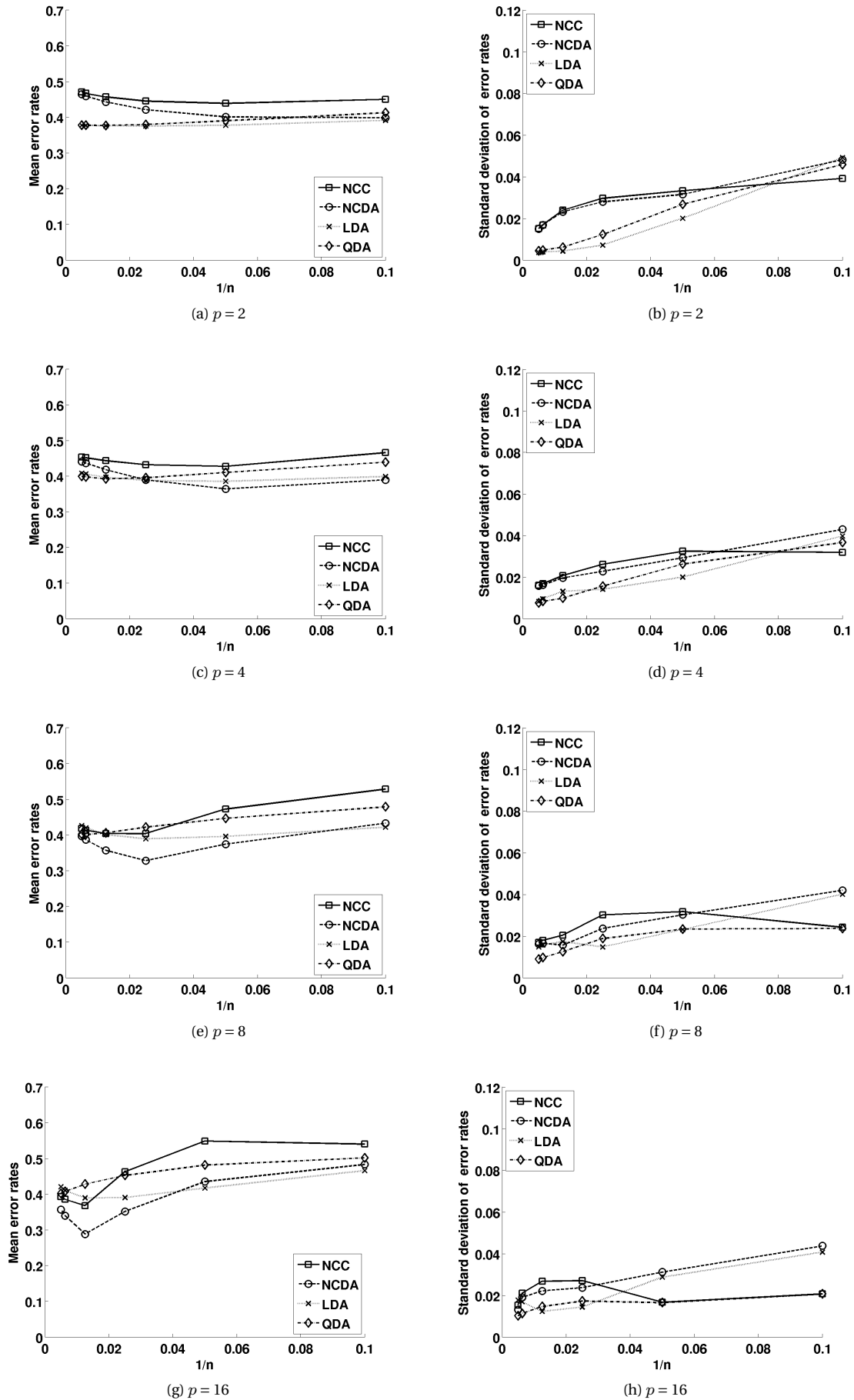


Figure 6: Experiment 3 (mixture of two Gaussians, $\mu_1 = \mu_2$, $\Sigma_1 = \Sigma_2 = I$): Mean (left) and standard deviation (right) of error rate under different p .